PROCEEDINGS OF SCIENCE

Update on testing of air-shower modelling using combined data of the Pierre Auger Observatory and phenomenological consequences

Jakub Vícha[a,*] **for the Pierre Auger Collaboration**[b]

[a] *FZU - Institute Of Physics of the Czech Academy of Sciences, Prague, Czech Republic*
[b] *Observatorio Pierre Auger, Av. San Martín Norte 304, 5613 Malargüe, Argentina*
Full author list: https://www.auger.org/archive/authors_icrc_2025.html

E-mail: spokespersons@auger.org

The combined data of Fluorescence and Surface Detectors of the Pierre Auger Observatory has recently provided the strongest constraints on the validity of predictions from current models of hadronic interactions. The unmodified predictions of these models on the depth of shower maximum ($X_{\rm max}$) and the hadronic part of the ground signal are unable to accurately describe the measured data at a level of more than 5σ in the energy range 3-10 EeV. This inconsistency has been shown to originate not only from the predicted amount of muons at the ground level, but also from the predicted scale of $X_{\rm max}$, which must be adjusted to better match the observed data. The resulting deeper $X_{\rm max}$ scales of the models imply a heavier mass composition to be interpreted from the $X_{\rm max}$ measurements.

We show the results of the test with an updated data set of the Pierre Auger Observatory, studying also the energy evolution of the fitted modification parameters and new versions of the models of hadronic interactions. Additionally, we discuss the phenomenological consequences of the deeper $X_{\rm max}$ scale of models on the interpretation of the features of the energy spectrum and the muon problem in air-shower modelling.

39th International Cosmic Ray Conference (ICRC2025)
15 – 24 July, 2025
Geneva, Switzerland

*Speaker

PoS(ICRC2025)431

1. Introduction

The combined data from the Surface and Fluorescence Detectors of the Pierre Auger Observatory [1] allow to put strong constraints on the predictions of models of hadronic interactions. The method of fitting two-dimensional histograms of the ground signal at 1000 m from the shower core and the depth of shower maximum, $X_{\rm max}$, has shown, for the first time, 5σ tension between the prediction of hadronic interaction models EPOS-LHC [2], QGSJET II-04 [3], SIBYLL 2.3d [4] and measured data for energies 3-10 EeV [5]. The model predictions were assumed to be modified by mass and energy independent parameters $\Delta X_{\rm max}$ and $R_{\rm had}(\theta)$, shifting the predicted $X_{\rm max}$ scale and rescaling the hadronic part of the ground signal at 1000 m from the shower core, respectively. In this way, we removed the main differences between the model predictions. The data were shown to be best described when not only the hadronic part of the ground signal was increased by ≈(15-25)%, but also the predicted $X_{\rm max}$ scale was shifted deeper by ≈(20-50) g/cm^2. The fitted primary fractions of four primary species: protons (p), helium (He), oxygen (O), and iron (Fe) nuclei combine to a heavier mass composition than is usually estimated from the $X_{\rm max}$ fits to the unmodified model predictions [6]. We have also shown that in the case of the QGSJET II-04 model, there is a strong indication of too hard muon spectra generated by the model at 1000 m from the shower core.

In this proceedings, we present an update of the method applied to newer data than in [5] with an extended energy range $10^{18.4-19.5}$ eV, and we test new versions of the models of hadronic interactions: EPOS-LHC-R [7], QGSJET III-01 [8] and slightly modified model SIBYLL 2.3e. We also test for the energy dependence of the modification parameters and indicate phenomenological consequences about the energy spectra and muon scale.

2. Testing New Models of Hadronic Interactions

We follow the high-quality selection of combined Surface and Fluorescence Detector data as in [5] extended by about 20% more events in the energy range $10^{18.5-19.0}$ eV, collected from 1st January 2004 up to 31st December 2021. On top of this benchmark energy range with 2740 events, we extend our analysis to energy ranges $10^{18.4-18.5}$ eV, $10^{18.5-18.7}$ eV, $10^{18.7-19.0}$ eV and $10^{19.0-19.5}$ eV with 1407, 1670, 1070 and 516 events, respectively, to study a possibility of an energy dependence of modification parameters. Monte Carlo simulations were produced using CORSIKA 7.8010 [9–11] and the detector simulation and shower reconstructions were processed using the Auger Offline code [12].

We show in Fig. 1 and Fig. 2 the resulting modification parameters of the simulated templates, and their correlations, after application of the log-likelihood fit described in [5] for the benchmark energy range. The primary fractions (see the right panel of Fig. 2) obtained using the new model versions are compatible with the values found for the older versions in [5], despite the large differences in predictions of the old and new versions of models QGSJET and EPOS.

The model SIBYLL 2.3e shows compatible value of $\Delta X_{\rm max}$ as for SIBYLL 2.3d in [5], as expected, but the needed rescaling of the hadronic part of the ground signal is now by 5-10% larger, mainly as a consequence of improvements applied in the reconstruction of the Surface Detector signal.

There are large changes in the predictions on air-shower properties in the case of the updated QGSJET model, including deeper $X_{\rm max}$ predictions for protons by ≈ 15 g/cm^2, while for iron nuclei

PoS(ICRC2025)431

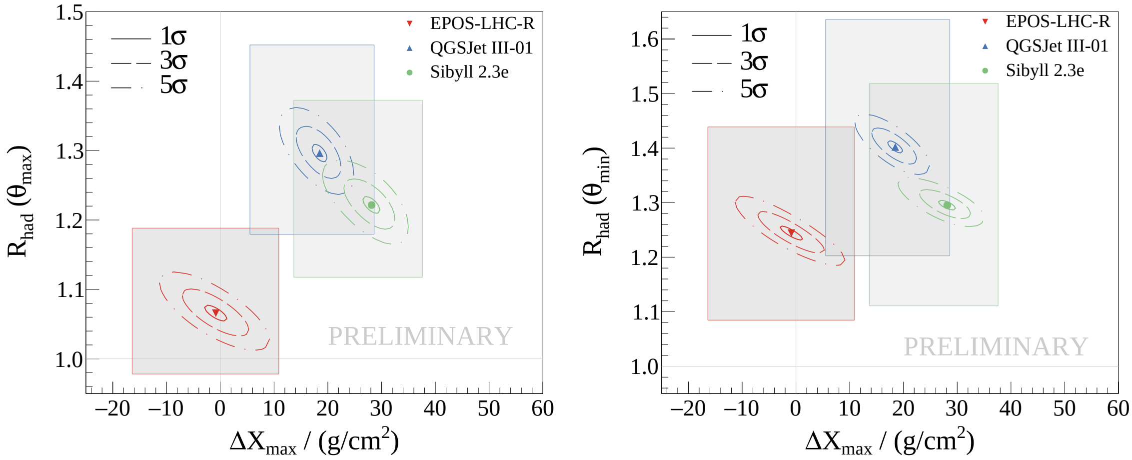

Figure 1: Correlations between $\Delta X_{\rm max}$ and $R_{\rm had}(\theta_{\rm max} \approx 55°)$ (left) and $R_{\rm had}(\theta_{\rm min} \approx 28°)$ (right) modifications of the model predictions obtained from the data fits in the energy range $10^{18.5-19.0}$ eV. The contours correspond to 1σ, 3σ, and 5σ statistical uncertainties. The gray rectangles are the projections of the total systematic uncertainties.

by ≈ 25 g/cm^2. The $X_{\rm max}$ fluctuations for iron nuclei in this model are now at the level of the total defragmentation of the nucleus, which was previously pointed out by [13] as a bug in the model Epos-LHC, and was fixed in the new Epos version. As a consequence, the fitted $X_{\rm max}$ shift for QGSJet III-01 is now smaller than in [5] for QGSJet II-04, being at the level of 20 g/cm^{2}only, however, the hadronic signal at 1000 m needs to be increased by a larger value at the level of 30-40%.

The best performing model, in general, is the Epos-LHC-R model with the predicted $X_{\rm max}$ scale compatible according to the test. However, there are large differences in the hadronic rescaling at the two extreme zenith angles (see the left panel of Fig. 2), strongly indicating that the predicted muon spectra at 1000 m from the shower core are too hard than what is measured, and the hardest among the studied models.

We have also tested possible energy dependence of modification parameters, see Fig. 3 for $\Delta X_{\rm max}$, by dividing the measured data into multiple ranges of energy. Given the available event statistics, the benchmark values of $\Delta X_{\rm max}$ obtained in the energy range $10^{18.5-19.0}$ eV were found compatible with the values for other energy ranges for all three models. Similar results were found for the two values of $R_{\rm had}(\theta)$. This finding supports the assumption of mass-independent modification parameters, which would be otherwise expected to manifest through the energy-per-nucleon scaling as a consequence of the Superposition model [14]. Our specific searches for mass dependencies of modification parameters further support this claim. From data on $\Delta X_{\rm max}$ we can not also exclude a mild energy dependence in the studied energy range given the available statistics. However, such an effect is expected for the energy evolution of $\langle \ln A \rangle$ by ≈ 1 [15] between $10^{18.4-19.5}$ eV, which affects the mass-dependent bias on $\Delta X_{\rm max}$ coming from the method itself as it was shown in Fig. 12 in [5] for the older versions of models. We illustrate estimation of such an effect using gray lines corresponding to the change of $\Delta X_{\rm max}$ bias by 4 ± 1 g/cm^{2}per decade of energy in Fig. 3.

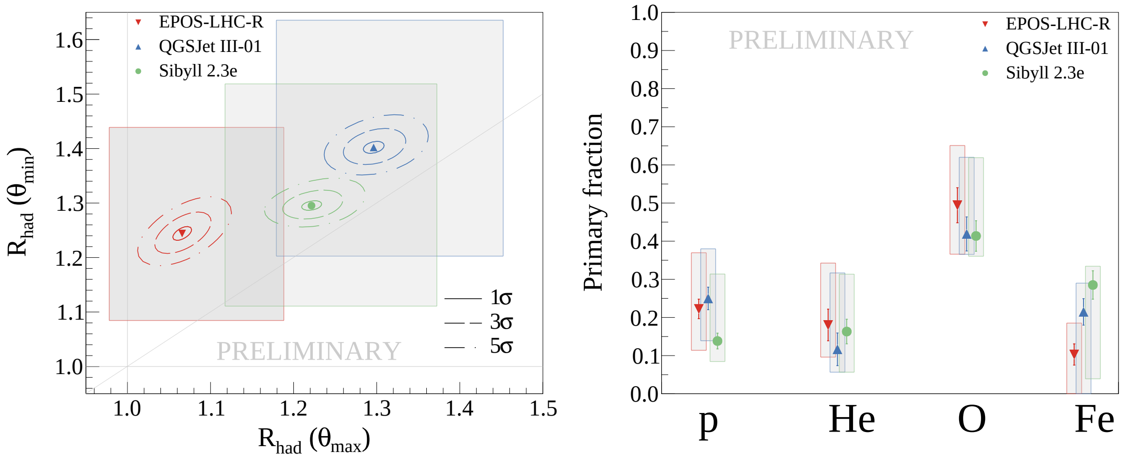

Figure 2: Left panel: Correlations between $R_{had}(\theta_{max} \approx 55°)$ and $R_{had}(\theta_{min} \approx 28°)$ modifications of the model predictions obtained from the data fits in the energy range $10^{18.5-19.0}$ eV. The contours correspond to 1σ, 3σ, and 5σ statistical uncertainties. The gray rectangles are the projections of the total systematic uncertainties. Right panel: The most likely primary fractions of the four components from the data fits using ΔX_{max} and $R_{had}(\theta)$. The height of the gray bands shows the size of projected total systematic uncertainties.

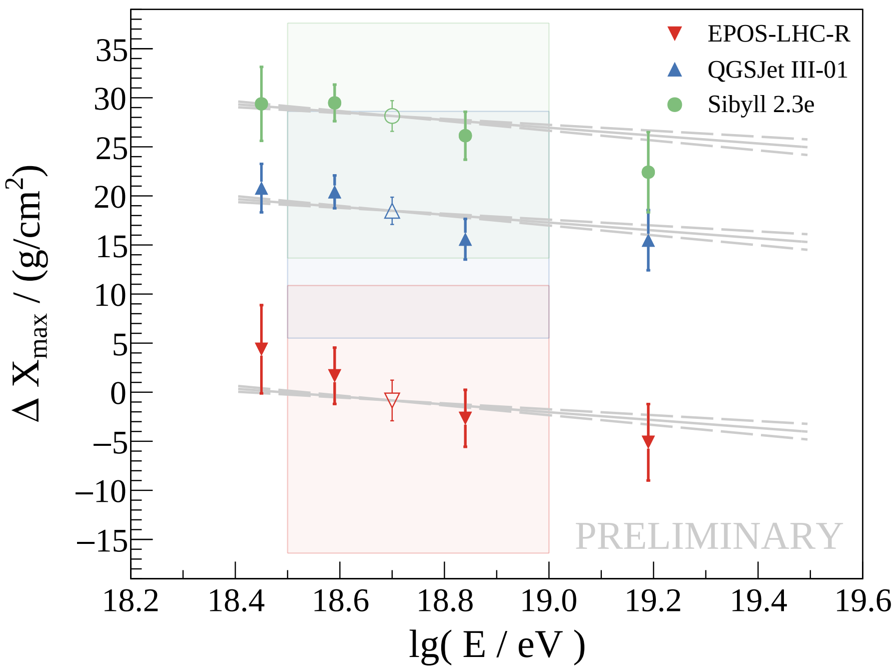

Figure 3: The fitted values of the ΔX_{max} parameter for various selections of energy range. The benchmark energy bin (open markers) contains also the bands of the projected systematic uncertainties. The expected systematic effect of the method (4 ± 1) g/cm^{2}per decade of energy is shown by gray lines.

Table 1: The $\Delta X_{\max}$ values with statistical and systematical uncertainties found for older versions of hadronic interaction models in [5] and here for the new models in the energy range $10^{18.5-19.0}$ eV.

	EPOS-LHC	QGSJET II-04	SIBYLL 2.3d
$\Delta X_{\max}$ / (g/cm^2)	$22 \pm 3\,^{+11}_{-14}$	$47^{+2}_{-1}\,^{+9}_{-11}$	$29 \pm 2\,^{+10}_{-13}$
	EPOS-LHC-R	QGSJET III-01	SIBYLL 2.3e
$\Delta X_{\max}$ / (g/cm^2)	$-1 \pm 2\,^{+12}_{-16}$	$18 \pm 1\,^{+10}_{-13}$	$28 \pm 2\,^{+9}_{-14}$

3. Phenomenology Consequences of Deeper Scale of $X_{\max}$

Given the non-observation of dependencies of modification parameters on energy or mass, we show in Fig. 4 the primary fractions obtained by fitting the $X_{\max}$ distributions [16] using modified simulation templates by $\Delta X_{\max}$ from the Table 1 for older and newer versions of the models, without taking statistical and systematic uncertainties into account. Note the N and Fe nuclei represent groups for nuclei of similar masses. Under the assumption of a constant $\Delta X_{\max}$ modification in models, we see a general trend of suppression of protons and helium nuclei beyond the ankle energy ($\approx$ 5 EeV). An increase of the nitrogen fraction between the ankle and instep ($\approx$ 13 EeV) energy [17] is also noticeable for all modified model predictions. In case of the iron nuclei, an increase of the relative fraction towards the highest energies is common for all predictions of modified models.

In Fig. 5, we multiply the total energy spectrum from [18] by the primary fractions obtained in Fig. 4. It illustrates that despite a global shift towards deeper predictions on $X_{\max}$ with the new models, the remaining differences in other model predictions like $X_{\max}$ fluctuations or p-Fe difference in $\langle X_{\max} \rangle$ even increased. As a consequence, there is no convergence in the interpreted mass composition and thus of the individual energy spectra. However, the connection between the instep feature in the energy spectrum and the start of fading of nitrogen nuclei from the beam, as proposed in [19], seems to be a common feature of all the model predictions, if the predicted $X_{\max}$ scale is shifted by $\Delta X_{\max}$. Note that this interpretation of instep as a transition between the dominance of different mass groups is consistent with what was found in [20], where the instep feature was attributed to the change in dominance of He to N nuclei due to injection and propagation effect.

Finally, we illustrate the alleviation of the muon problem in Fig. 6 for the measurement in [21] for zenith angles $62^\circ \leq \theta \leq 80^\circ$. The original model predictions (dashed lines) are also shifted for $\Delta X_{\max}$ obtained in [5]. The underestimation of the muon scale in the models is then reduced to about 15-25%, which is in line with the values obtained in [5] for the zenith angles $\theta \leq 60^\circ$. The new model EPOS-LHC-R predicts more muons at larger zenith angles than its previous version, therefore better compatibility with measurement of the muon size in inclined showers is expected.

4. Summary

The powerful combination of Surface and Fluorescence Detectors of the Pierre Auger Observatory allowed to test new versions of three models of hadronic interactions EPOS-LHC-R, QGSJET III-01 and SIBYLL 2.3e using the method from [5]. Although an improvement in the description of the measured $X_{\max}$ scale has been observed in the new versions of EPOS and QGSJET,

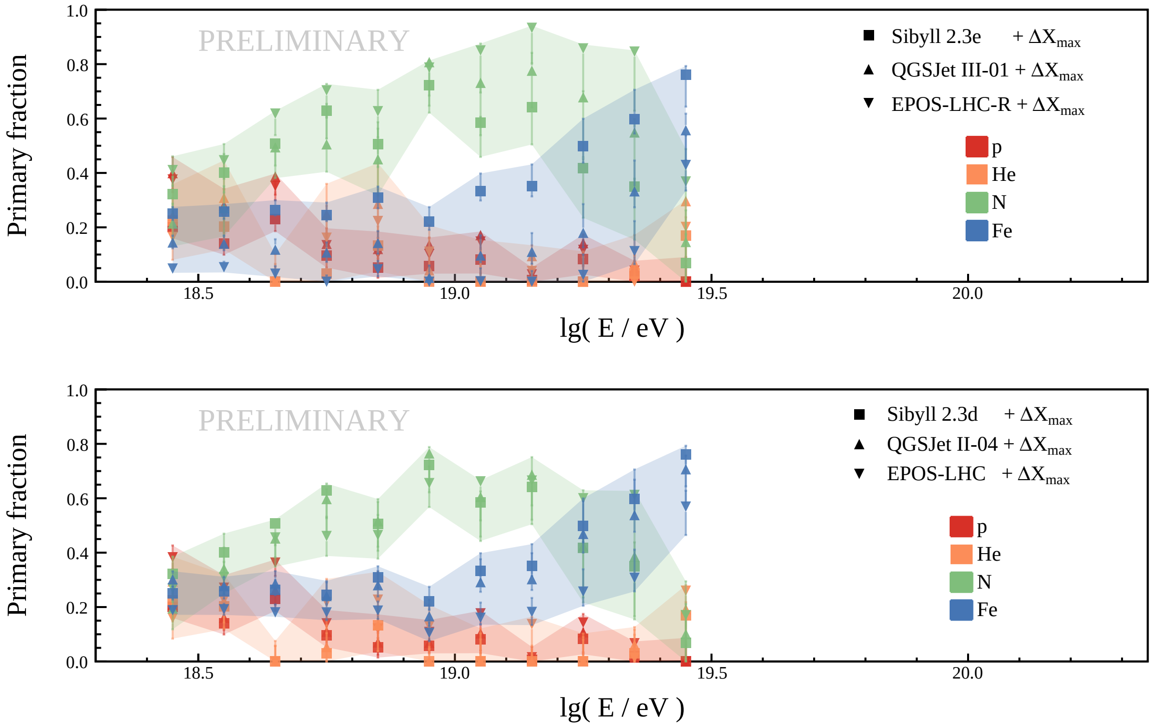

Figure 4: The energy evolutions of four primary fractions fitted to the X_{max} distributions using modified templates by ΔX_{max} for older (bottom panel) and new (top panel) versions of the hadronic interaction models.

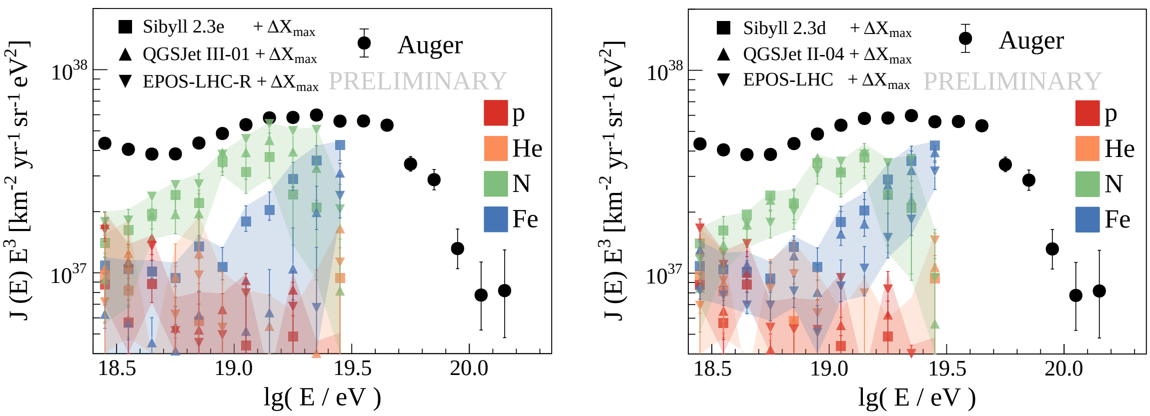

Figure 5: The total energy spectrum measured by the Pierre Auger Observatory [18] decomposed into four primary components using relative primary fractions shown in Fig. 4 for older (right panel) and new (left panel) versions of the hadronic interaction models.

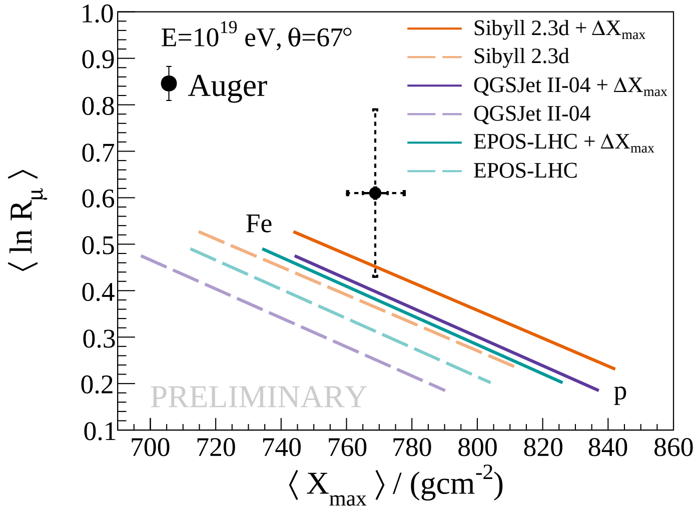

Figure 6: The muon scale (R_μ) vs. $X_{\rm max}$ measurement at the Pierre Auger Observatory using inclined showers at energy ~10 EeV from [21]. We estimate predictions between p and Fe nuclei for original models of hadronic interactions (dashed lines) and for their shifted $X_{\rm max}$ predictions by $\Delta X_{\rm max}$ (full lines).

all models are still unable to describe the measured data satisfactorily well in the energy range $10^{18.5-19.0}$ eV. All models seem to predict too hard spectra of muons causing less steep attenuation of the hadronic signal than is favored by the data. Yet, interestingly, the primary fractions found to best describe the measurements are consistent between the older and new versions of the models, when $\Delta X_{\rm max}$ and $R_{\rm had}(\theta)$ modifications of the simulated templates are assumed.

The results of our studies in various energy ranges are compatible with no energy dependence of the modification parameters in the energy range $10^{18.4-19.5}$ eV, which brings us to probe some basic phenomenology consequences regarding the energy spectrum and the lack of predicted muon scale compared to the direct measurement. For that, we assume a constant $\Delta X_{\rm max}$ offset obtained in $10^{18.5-19.0}$ eV and apply it in the model predictions on $X_{\rm max}$ to the full energy range $10^{18.4-19.5}$ eV. As a consequence of this assumption, for all models the protons and helium nuclei seem to be suppressed above the ankle energy. The nitrogen nuclei increase their fraction in the primary beam above this energy up to the instep feature and start to steeply fade just beyond this energy. Iron nuclei seem to increase their abundance towards the highest energies. In case of the $\Delta X_{\rm max}$ modifications, the problem of models from direct muon measurements at 10 EeV is alleviated to the level of 15-25% for older versions of the models, consistent with the result of [5] at lower energy and zenith angles.

References

[1] Pierre Auger collaboration, *The Pierre Auger Cosmic Ray Observatory*, *NIM A* **798** (2015) 172 .

[2] T. Pierog, I. Karpenko, J.M. Katzy, E. Yatsenko and K. Werner, *EPOS LHC: Test of collective hadronization with data measured at the cern large hadron collider*, *PRC* **92** (2015) 034906.

[3] S. Ostapchenko, *Monte Carlo treatment of hadronic interactions in enhanced Pomeron scheme: QGSJET-II model*, *PRD* **83** (2011) 014018.

[4] F. Riehn, R. Engel, A. Fedynitch, T.K. Gaisser and T. Stanev, *Hadronic interaction model Sibyll 2.3d and extensive air showers*, *PRD* **102** (2020) 063002.

[5] Pierre Auger collaboration, *Testing hadronic-model predictions of depth of maximum of air-shower profiles and ground-particle signals using hybrid data of the Pierre Auger Observatory*, *PRD* **109** (2024) 102001.

[6] Pierre Auger collaboration, *Depth of maximum of air-shower profiles at the Pierre Auger Observatory. II. Composition implications*, *PRD* **90** (2014) 122006.

[7] T. Pierog and K. Werner, *EPOS LHC-R : up-to-date hadronic model for EAS simulations*, *PoS(ICRC2023)230* .

[8] S. Ostapchenko, *QGSJET-III model of high energy hadronic interactions. II. Particle production and extensive air shower characteristics*, *PRD* **109** (2024) 094019.

[9] D. Heck, J. Knapp, J.N. Capdevielle, G. Schatz and T. Thouw, *CORSIKA: A Monte Carlo code to simulate extensive air showers*, *Report FZKA Forschungszentrum Karlsruhe* **6019** (1998) .

[10] D. Heck and J. Knapp, *Upgrade of the Monte Carlo code CORSIKA to simulate extensive air showers with energies* > 10^{20} *eV*, *Report FZKA Forschungszentrum Karlsruhe* **6097** (1998) .

[11] D. Heck, *Air shower simulation with CORSIKA at arbitrary direction of incidence*, *Report FZKA Forschungszentrum Karlsruhe* **7254** (2006) .

[12] S. Argirò, S. Barroso, J. Gonzalez, L. Nellen, T. Paul, T. Porter et al., *The offline software framework of the Pierre Auger Observatory*, *NIM A* **580** (2007) 1485.

[13] S. Ostapchenko, *High Energy Cosmic Ray Interactions and UHECR Composition Problem, talk at the UHECR 2018, Paris, October 08-12, 2018 (Paris)*, 2018 (accessed Oct, 2018).

[14] J. Engel, T.K. Gaisser, P. Lipari and T. Stanev, *Nucleus-nucleus collisions and interpretation of cosmic-ray cascades*, *PRD* **46** (1992) 5013.

[15] Pierre Auger Collaboration collaboration, *Depth of maximum of air-shower profiles at the Pierre Auger Observatory. I. Measurements at energies above* $10^{17.8}$ *eV*, *PRD* **90** (2014) 122005.

[16] E. Mayotte, *Measurement and Interpretation of UHECR Mass Composition at the Pierre Auger Observatory*, in *Proceedings of 39th International Cosmic Ray Conference — PoS(ICRC2025)*, vol. XXX, p. YYY, 2025.

[17] The Pierre Auger collaboration, *Features of the Energy Spectrum of Cosmic Rays above* 2.5×10^{18} eV *Using the Pierre Auger Observatory*, *PRL* **125** (2020) 121106.

[18] Pierre Auger collaboration, *Measurement of the cosmic-ray energy spectrum above* 2.5×10^{18} eV *using the Pierre Auger Observatory*, *PRD* **102** (2020) 062005.

[19] J. Vícha et al., *A Heavy-Metal Scenario of Ultra-High-Energy Cosmic Rays*, *accepted in ApJL* (2025) [2504.11985].

[20] The Pierre Auger collaboration, *Constraining the sources of ultra-high-energy cosmic rays across and above the ankle with the spectrum and composition data measured at the Pierre Auger Observatory*, *JCAP* **2023** (2023) 024.

[21] The Pierre Auger collaboration, *Measurement of the Fluctuations in the Number of Muons in Extensive Air Showers with the Pierre Auger Observatory*, *PRL* **126** (2021) 152002.

The Pierre Auger Collaboration

PIERRE AUGER OBSERVATORY

A. Abdul Halim[13], P. Abreu[70], M. Aglietta[53,51], I. Allekotte[1], K. Almeida Cheminant[78,77], A. Almela[7,12], R. Aloisio[44,45], J. Alvarez-Muñiz[76], A. Ambrosone[44], J. Ammerman Yebra[76], G.A. Anastasi[57,46], L. Anchordoqui[83], B. Andrada[7], L. Andrade Dourado[44,45], S. Andringa[70], L. Apollonio[58,48], C. Aramo[49], E. Arnone[62,51], J.C. Arteaga Velázquez[66], P. Assis[70], G. Avila[11], E. Avocone[56,45], A. Bakalova[31], F. Barbato[44,45], A. Bartz Mocellin[82], J.A. Bellido[13], C. Berat[35], M.E. Bertaina[62,51], M. Bianciotto[62,51], P.L. Biermann[a], V. Binet[5], K. Bismark[38,7], T. Bister[77,78], J. Biteau[36,i], J. Blazek[31], J. Blümer[40], M. Boháčová[31], D. Boncioli[56,45], C. Bonifazi[8], L. Bonneau Arbeletche[22], N. Borodai[68], J. Brack[f], P.G. Brichetto Orchera[7,40], F.L. Briechle[41], A. Bueno[75], S. Buitink[15], M. Buscemi[46,57], M. Büsken[38,7], A. Bwembya[77,78], K.S. Caballero-Mora[65], S. Cabana-Freire[76], L. Caccianiga[58,48], F. Campuzano[6], J. Caraça-Valente[82], R. Caruso[57,46], A. Castellina[53,51], F. Catalani[19], G. Cataldi[47], L. Cazon[76], M. Cerda[10], B. Čermáková[40], A. Cermenati[44,45], J.A. Chinellato[22], J. Chudoba[31], L. Chytka[32], R.W. Clay[13], A.C. Cobos Cerutti[6], R. Colalillo[59,49], R. Conceição[70], G. Consolati[48,54], M. Conte[55,47], F. Convenga[44,45], D. Correia dos Santos[27], P.J. Costa[70], C.E. Covault[81], M. Cristinziani[43], C.S. Cruz Sanchez[3], S. Dasso[4,2], K. Daumiller[40], B.R. Dawson[13], R.M. de Almeida[27], E.-T. de Boone[43], B. de Errico[27], J. de Jesús[7], S.J. de Jong[77,78], J.R.T. de Mello Neto[27], I. De Mitri[44,45], J. de Oliveira[18], D. de Oliveira Franco[42], F. de Palma[55,47], V. de Souza[20], E. De Vito[55,47], A. Del Popolo[57,46], O. Deligny[33], N. Denner[31], L. Deval[53,51], A. di Matteo[51], C. Dobrigkeit[22], J.C. D'Olivo[67], L.M. Domingues Mendes[16,70], Q. Dorosti[43], J.C. dos Anjos[16], R.C. dos Anjos[26], J. Ebr[31], F. Ellwanger[40], R. Engel[38,40], I. Epicoco[55,47], M. Erdmann[41], A. Etchegoyen[7,12], C. Evoli[44,45], H. Falcke[77,79,78], G. Farrar[85], A.C. Fauth[22], T. Fehler[43], F. Feldbusch[39], A. Fernandes[70], M. Fernandez[14], B. Fick[84], J.M. Figueira[7], P. Filip[38,7], A. Filipčič[74,73], T. Fitoussi[40], B. Flaggs[87], T. Fodran[77], A. Franco[47], M. Freitas[70], T. Fujii[86,h], A. Fuster[7,12], C. Galea[77], B. García[6], C. Gaudu[37], P.L. Ghia[33], U. Giaccari[47], F. Gobbi[10], F. Gollan[7], G. Golup[1], M. Gómez Berisso[1], P.F. Gómez Vitale[11], J.P. Gongora[11], J.M. González[1], N. González[7], D. Góra[68], A. Gorgi[53,51], M. Gottowik[40], F. Guarino[59,49], G.P. Guedes[23], L. Gülzow[40], S. Hahn[38], P. Hamal[31], M.R. Hampel[7], P. Hansen[3], V.M. Harvey[13], A. Haungs[40], T. Hebbeker[41], C. Hojvat[d], J.R. Hörandel[77,78], P. Horvath[32], M. Hrabovský[32], T. Huege[40,15], A. Insolia[57,46], P.G. Isar[72], M. Ismaiel[77,78], P. Janecek[31], V. Jilek[31], K.-H. Kampert[37], B. Keilhauer[40], A. Khakurdikar[77], V.V. Kizakke Covilakam[7,40], H.O. Klages[40], M. Kleifges[39], J. Köhler[40], F. Krieger[41], M. Kubatova[31], N. Kunka[39], B.L. Lago[17], N. Langner[41], N. Leal[7], M.A. Leigui de Oliveira[25], Y. Lema-Capeans[76], A. Letessier-Selvon[34], I. Lhenry-Yvon[33], L. Lopes[70], J.P. Lundquist[73], M. Mallamaci[60,46], D. Mandat[31], P. Mantsch[d], F.M. Mariani[58,48], A.G. Mariazzi[3], I.C. Mariş[14], G. Marsella[60,46], D. Martello[55,47], S. Martinelli[40,7], M.A. Martins[76], H.-J. Mathes[40], J. Matthews[g], G. Matthiae[61,50], E. Mayotte[82], S. Mayotte[82], P.O. Mazur[d], G. Medina-Tanco[67], J. Meinert[37], D. Melo[7], A. Menshikov[39], C. Merx[40], S. Michal[31], M.I. Micheletti[5], L. Miramonti[58,48], M. Mogarkar[68], S. Mollerach[1], F. Montanet[35], L. Morejon[37], K. Mulrey[77,78], R. Mussa[51], W.M. Namasaka[37], S. Negi[31], L. Nellen[67], K. Nguyen[84], G. Nicora[9], M. Niechciol[43], D. Nitz[84], D. Nosek[30], A. Novikov[87], V. Novotny[30], L. Nožka[32], A. Nucita[55,47], L.A. Núñez[29], J. Ochoa[7,40], C. Oliveira[20], L. Östman[31], M. Palatka[31], J. Pallotta[9], S. Panja[31], G. Parente[76], T. Paulsen[37], J. Pawlowsky[37], M. Pech[31], J. Pękala[68], R. Pelayo[64], V. Pelgrims[14], L.A.S. Pereira[24], E.E. Pereira Martins[38,7], C. Pérez Bertolli[7,40], L. Perrone[55,47], S. Petrera[44,45], C. Petrucci[56], T. Pierog[40], M. Pimenta[70], M. Platino[7], B. Pont[77], M. Pourmohammad Shahvar[60,46], P. Privitera[86], C. Priyadarshi[68], M. Prouza[31], K. Pytel[69], S. Querchfeld[37], J. Rautenberg[37], D. Ravignani[7], J.V. Reginatto Akim[22], A. Reuzki[41], J. Ridky[31], F. Riehn[76,j], M. Risse[43], V. Rizi[56,45], E. Rodriguez[7,40], G. Rodriguez Fernandez[50], J. Rodriguez Rojo[11], S. Rossoni[42], M. Roth[40], E. Roulet[1], A.C. Rovero[4], A. Saftoiu[71], M. Saharan[77], F. Salamida[56,45], H. Salazar[63], G. Salina[50], P. Sampathkumar[40], N. San Martin[82], J.D. Sanabria Gomez[29], F. Sánchez[7], E.M. Santos[21], E. Santos[31], F. Sarazin[82], R. Sarmento[70], R. Sato[11], P. Savina[44,45], V. Scherini[55,47], H. Schieler[40], M. Schimassek[33], M. Schimp[37], D. Schmidt[40], O. Scholten[15,b], H. Schoorlemmer[77,78], P. Schovánek[31], F.G. Schröder[87,40],

J. Schulte[41], T. Schulz[31], S.J. Sciutto[3], M. Scornavacche[7], A. Sedoski[7], A. Segreto[52,46], S. Sehgal[37], S.U. Shivashankara[73], G. Sigl[42], K. Simkova[15,14], F. Simon[39], R. Šmída[86], P. Sommers[e], R. Squartini[10], M. Stadelmaier[40,48,58], S. Stanič[73], J. Stasielak[68], P. Stassi[35], S. Strähnz[38], M. Straub[41], T. Suomijärvi[36], A.D. Supanitsky[7], Z. Svozilikova[31], K. Syrokvas[30], Z. Szadkowski[69], F. Tairli[13], M. Tambone[59,49], A. Tapia[28], C. Taricco[62,51], C. Timmermans[78,77], O. Tkachenko[31], P. Tobiska[31], C.J. Todero Peixoto[19], B. Tomé[70], A. Travaini[10], P. Travnicek[31], M. Tueros[3], M. Unger[40], R. Uzeiroska[37], L. Vaclavek[32], M. Vacula[32], I. Vaiman[44,45], J.F. Valdés Galicia[67], L. Valore[59,49], P. van Dillen[77,78], E. Varela[63], V. Vašíčková[37], A. Vásquez-Ramírez[29], D. Veberič[40], I.D. Vergara Quispe[3], S. Verpoest[87], V. Verzi[50], J. Vicha[31], J. Vink[80], S. Vorobiov[73], J.B. Vuta[31], C. Watanabe[27], A.A. Watson[c], A. Weindl[40], M. Weitz[37], L. Wiencke[82], H. Wilczyński[68], B. Wundheiler[7], B. Yue[37], A. Yushkov[31], E. Zas[76], D. Zavrtanik[73,74], M. Zavrtanik[74,73]

[1] Centro Atómico Bariloche and Instituto Balseiro (CNEA-UNCuyo-CONICET), San Carlos de Bariloche, Argentina
[2] Departamento de Física and Departamento de Ciencias de la Atmósfera y los Océanos, FCEyN, Universidad de Buenos Aires and CONICET, Buenos Aires, Argentina
[3] IFLP, Universidad Nacional de La Plata and CONICET, La Plata, Argentina
[4] Instituto de Astronomía y Física del Espacio (IAFE, CONICET-UBA), Buenos Aires, Argentina
[5] Instituto de Física de Rosario (IFIR) – CONICET/U.N.R. and Facultad de Ciencias Bioquímicas y Farmacéuticas U.N.R., Rosario, Argentina
[6] Instituto de Tecnologías en Detección y Astropartículas (CNEA, CONICET, UNSAM), and Universidad Tecnológica Nacional – Facultad Regional Mendoza (CONICET/CNEA), Mendoza, Argentina
[7] Instituto de Tecnologías en Detección y Astropartículas (CNEA, CONICET, UNSAM), Buenos Aires, Argentina
[8] International Center of Advanced Studies and Instituto de Ciencias Físicas, ECyT-UNSAM and CONICET, Campus Miguelete – San Martín, Buenos Aires, Argentina
[9] Laboratorio Atmósfera – Departamento de Investigaciones en Láseres y sus Aplicaciones – UNIDEF (CITEDEF-CONICET), Argentina
[10] Observatorio Pierre Auger, Malargüe, Argentina
[11] Observatorio Pierre Auger and Comisión Nacional de Energía Atómica, Malargüe, Argentina
[12] Universidad Tecnológica Nacional – Facultad Regional Buenos Aires, Buenos Aires, Argentina
[13] University of Adelaide, Adelaide, S.A., Australia
[14] Université Libre de Bruxelles (ULB), Brussels, Belgium
[15] Vrije Universiteit Brussels, Brussels, Belgium
[16] Centro Brasileiro de Pesquisas Fisicas, Rio de Janeiro, RJ, Brazil
[17] Centro Federal de Educação Tecnológica Celso Suckow da Fonseca, Petropolis, Brazil
[18] Instituto Federal de Educação, Ciência e Tecnologia do Rio de Janeiro (IFRJ), Brazil
[19] Universidade de São Paulo, Escola de Engenharia de Lorena, Lorena, SP, Brazil
[20] Universidade de São Paulo, Instituto de Física de São Carlos, São Carlos, SP, Brazil
[21] Universidade de São Paulo, Instituto de Física, São Paulo, SP, Brazil
[22] Universidade Estadual de Campinas (UNICAMP), IFGW, Campinas, SP, Brazil
[23] Universidade Estadual de Feira de Santana, Feira de Santana, Brazil
[24] Universidade Federal de Campina Grande, Centro de Ciencias e Tecnologia, Campina Grande, Brazil
[25] Universidade Federal do ABC, Santo André, SP, Brazil
[26] Universidade Federal do Paraná, Setor Palotina, Palotina, Brazil
[27] Universidade Federal do Rio de Janeiro, Instituto de Física, Rio de Janeiro, RJ, Brazil
[28] Universidad de Medellín, Medellín, Colombia
[29] Universidad Industrial de Santander, Bucaramanga, Colombia
[30] Charles University, Faculty of Mathematics and Physics, Institute of Particle and Nuclear Physics, Prague, Czech Republic

PoS(ICRC2025)431

[31] Institute of Physics of the Czech Academy of Sciences, Prague, Czech Republic
[32] Palacky University, Olomouc, Czech Republic
[33] CNRS/IN2P3, IJCLab, Université Paris-Saclay, Orsay, France
[34] Laboratoire de Physique Nucléaire et de Hautes Energies (LPNHE), Sorbonne Université, Université de Paris, CNRS-IN2P3, Paris, France
[35] Univ. Grenoble Alpes, CNRS, Grenoble Institute of Engineering Univ. Grenoble Alpes, LPSC-IN2P3, 38000 Grenoble, France
[36] Université Paris-Saclay, CNRS/IN2P3, IJCLab, Orsay, France
[37] Bergische Universität Wuppertal, Department of Physics, Wuppertal, Germany
[38] Karlsruhe Institute of Technology (KIT), Institute for Experimental Particle Physics, Karlsruhe, Germany
[39] Karlsruhe Institute of Technology (KIT), Institut für Prozessdatenverarbeitung und Elektronik, Karlsruhe, Germany
[40] Karlsruhe Institute of Technology (KIT), Institute for Astroparticle Physics, Karlsruhe, Germany
[41] RWTH Aachen University, III. Physikalisches Institut A, Aachen, Germany
[42] Universität Hamburg, II. Institut für Theoretische Physik, Hamburg, Germany
[43] Universität Siegen, Department Physik – Experimentelle Teilchenphysik, Siegen, Germany
[44] Gran Sasso Science Institute, L'Aquila, Italy
[45] INFN Laboratori Nazionali del Gran Sasso, Assergi (L'Aquila), Italy
[46] INFN, Sezione di Catania, Catania, Italy
[47] INFN, Sezione di Lecce, Lecce, Italy
[48] INFN, Sezione di Milano, Milano, Italy
[49] INFN, Sezione di Napoli, Napoli, Italy
[50] INFN, Sezione di Roma "Tor Vergata", Roma, Italy
[51] INFN, Sezione di Torino, Torino, Italy
[52] Istituto di Astrofisica Spaziale e Fisica Cosmica di Palermo (INAF), Palermo, Italy
[53] Osservatorio Astrofisico di Torino (INAF), Torino, Italy
[54] Politecnico di Milano, Dipartimento di Scienze e Tecnologie Aerospaziali , Milano, Italy
[55] Università del Salento, Dipartimento di Matematica e Fisica "E. De Giorgi", Lecce, Italy
[56] Università dell'Aquila, Dipartimento di Scienze Fisiche e Chimiche, L'Aquila, Italy
[57] Università di Catania, Dipartimento di Fisica e Astronomia "Ettore Majorana", Catania, Italy
[58] Università di Milano, Dipartimento di Fisica, Milano, Italy
[59] Università di Napoli "Federico II", Dipartimento di Fisica "Ettore Pancini", Napoli, Italy
[60] Università di Palermo, Dipartimento di Fisica e Chimica "E. Segrè", Palermo, Italy
[61] Università di Roma "Tor Vergata", Dipartimento di Fisica, Roma, Italy
[62] Università Torino, Dipartimento di Fisica, Torino, Italy
[63] Benemérita Universidad Autónoma de Puebla, Puebla, México
[64] Unidad Profesional Interdisciplinaria en Ingeniería y Tecnologías Avanzadas del Instituto Politécnico Nacional (UPIITA-IPN), México, D.F., México
[65] Universidad Autónoma de Chiapas, Tuxtla Gutiérrez, Chiapas, México
[66] Universidad Michoacana de San Nicolás de Hidalgo, Morelia, Michoacán, México
[67] Universidad Nacional Autónoma de México, México, D.F., México
[68] Institute of Nuclear Physics PAN, Krakow, Poland
[69] University of Łódź, Faculty of High-Energy Astrophysics,Łódź, Poland
[70] Laboratório de Instrumentação e Física Experimental de Partículas – LIP and Instituto Superior Técnico – IST, Universidade de Lisboa – UL, Lisboa, Portugal
[71] "Horia Hulubei" National Institute for Physics and Nuclear Engineering, Bucharest-Magurele, Romania
[72] Institute of Space Science, Bucharest-Magurele, Romania
[73] Center for Astrophysics and Cosmology (CAC), University of Nova Gorica, Nova Gorica, Slovenia

[74] Experimental Particle Physics Department, J. Stefan Institute, Ljubljana, Slovenia
[75] Universidad de Granada and C.A.F.P.E., Granada, Spain
[76] Instituto Galego de Física de Altas Enerxías (IGFAE), Universidade de Santiago de Compostela, Santiago de Compostela, Spain
[77] IMAPP, Radboud University Nijmegen, Nijmegen, The Netherlands
[78] Nationaal Instituut voor Kernfysica en Hoge Energie Fysica (NIKHEF), Science Park, Amsterdam, The Netherlands
[79] Stichting Astronomisch Onderzoek in Nederland (ASTRON), Dwingeloo, The Netherlands
[80] Universiteit van Amsterdam, Faculty of Science, Amsterdam, The Netherlands
[81] Case Western Reserve University, Cleveland, OH, USA
[82] Colorado School of Mines, Golden, CO, USA
[83] Department of Physics and Astronomy, Lehman College, City University of New York, Bronx, NY, USA
[84] Michigan Technological University, Houghton, MI, USA
[85] New York University, New York, NY, USA
[86] University of Chicago, Enrico Fermi Institute, Chicago, IL, USA
[87] University of Delaware, Department of Physics and Astronomy, Bartol Research Institute, Newark, DE, USA

—

[a] Max-Planck-Institut für Radioastronomie, Bonn, Germany
[b] also at Kapteyn Institute, University of Groningen, Groningen, The Netherlands
[c] School of Physics and Astronomy, University of Leeds, Leeds, United Kingdom
[d] Fermi National Accelerator Laboratory, Fermilab, Batavia, IL, USA
[e] Pennsylvania State University, University Park, PA, USA
[f] Colorado State University, Fort Collins, CO, USA
[g] Louisiana State University, Baton Rouge, LA, USA
[h] now at Graduate School of Science, Osaka Metropolitan University, Osaka, Japan
[i] Institut universitaire de France (IUF), France
[j] now at Technische Universität Dortmund and Ruhr-Universität Bochum, Dortmund and Bochum, Germany

Acknowledgments

The successful installation, commissioning, and operation of the Pierre Auger Observatory would not have been possible without the strong commitment and effort from the technical and administrative staff in Malargüe. We are very grateful to the following agencies and organizations for financial support:

Argentina – Comisión Nacional de Energía Atómica; Agencia Nacional de Promoción Científica y Tecnológica (ANPCyT); Consejo Nacional de Investigaciones Científicas y Técnicas (CONICET); Gobierno de la Provincia de Mendoza; Municipalidad de Malargüe; NDM Holdings and Valle Las Leñas; in gratitude for their continuing cooperation over land access; Australia – the Australian Research Council; Belgium – Fonds de la Recherche Scientifique (FNRS); Research Foundation Flanders (FWO), Marie Curie Action of the European Union Grant No. 101107047; Brazil – Conselho Nacional de Desenvolvimento Científico e Tecnológico (CNPq); Financiadora de Estudos e Projetos (FINEP); Fundação de Amparo à Pesquisa do Estado de Rio de Janeiro (FAPERJ); São Paulo Research Foundation (FAPESP) Grants No. 2019/10151-2, No. 2010/07359-6 and No. 1999/05404-3; Ministério da Ciência, Tecnologia, Inovações e Comunicações (MCTIC); Czech Republic – GACR 24-13049S, CAS LQ100102401, MEYS LM2023032, CZ.02.1.01/0.0/0.0/16_013/0001402, CZ.02.1.01/0.0/0.0/18_046/0016010 and CZ.02.1.01/0.0/0.0/17_049/0008422 and CZ.02.01.01/00/22_008/0004632; France – Centre de Calcul IN2P3/CNRS; Centre National de la Recherche Scientifique (CNRS); Conseil Régional Ile-de-France; Département Physique Nucléaire et Corpusculaire (PNC-IN2P3/CNRS); Département Sciences de l'Univers

(SDU-INSU/CNRS); Institut Lagrange de Paris (ILP) Grant No. LABEX ANR-10-LABX-63 within the Investissements d'Avenir Programme Grant No. ANR-11-IDEX-0004-02; Germany – Bundesministerium für Bildung und Forschung (BMBF); Deutsche Forschungsgemeinschaft (DFG); Finanzministerium Baden-Württemberg; Helmholtz Alliance for Astroparticle Physics (HAP); Helmholtz-Gemeinschaft Deutscher Forschungszentren (HGF); Ministerium für Kultur und Wissenschaft des Landes Nordrhein-Westfalen; Ministerium für Wissenschaft, Forschung und Kunst des Landes Baden-Württemberg; Italy – Istituto Nazionale di Fisica Nucleare (INFN); Istituto Nazionale di Astrofisica (INAF); Ministero dell'Università e della Ricerca (MUR); CETEMPS Center of Excellence; Ministero degli Affari Esteri (MAE), ICSC Centro Nazionale di Ricerca in High Performance Computing, Big Data and Quantum Computing, funded by European Union NextGenerationEU, reference code CN_00000013; México – Consejo Nacional de Ciencia y Tecnología (CONACYT) No. 167733; Universidad Nacional Autónoma de México (UNAM); PAPIIT DGAPA-UNAM; The Netherlands – Ministry of Education, Culture and Science; Netherlands Organisation for Scientific Research (NWO); Dutch national e-infrastructure with the support of SURF Cooperative; Poland – Ministry of Education and Science, grants No. DIR/WK/2018/11 and 2022/WK/12; National Science Centre, grants No. 2016/22/M/ST9/00198, 2016/23/B/ST9/01635, 2020/39/B/ST9/01398, and 2022/45/B/ST9/02163; Portugal – Portuguese national funds and FEDER funds within Programa Operacional Factores de Competitividade through Fundação para a Ciência e a Tecnologia (COMPETE); Romania – Ministry of Research, Innovation and Digitization, CNCS-UEFISCDI, contract no. 30N/2023 under Romanian National Core Program LAPLAS VII, grant no. PN 23 21 01 02 and project number PN-III-P1-1.1-TE-2021-0924/TE57/2022, within PNCDI III; Slovenia – Slovenian Research Agency, grants P1-0031, P1-0385, I0-0033, N1-0111; Spain – Ministerio de Ciencia e Innovación/Agencia Estatal de Investigación (PID2019-105544GB-I00, PID2022-140510NB-I00 and RYC2019-027017-I), Xunta de Galicia (CIGUS Network of Research Centers, Consolidación 2021 GRC GI-2033, ED431C-2021/22 and ED431F-2022/15), Junta de Andalucía (SOMM17/6104/UGR and P18-FR-4314), and the European Union (Marie Sklodowska-Curie 101065027 and ERDF); USA – Department of Energy, Contracts No. DE-AC02-07CH11359, No. DE-FR02-04ER41300, No. DE-FG02-99ER41107 and No. DE-SC0011689; National Science Foundation, Grant No. 0450696, and NSF-2013199; The Grainger Foundation; Marie Curie-IRSES/EPLANET; European Particle Physics Latin American Network; and UNESCO.